Microelectronic Engineering 87 (2010) 537–542

Contents lists available at ScienceDirect

Microelectronic Engineering

journal homepage: www.elsevier.com/locate/mee

The ultrasonic wedge/wedge bonding process investigated using in situ real-time amplitudes from laser vibrometer and integrated force sensor

H. Gaul [a,*], A. Shah [b], M. Mayer [b], Y. Zhou [b], M. Schneider-Ramelow [c], H. Reichl [a]

[a] *Forschungsschwerpunkt Technologien der Mikroperipherik, TU Berlin, Berlin, Germany*
[b] *University of Waterloo, Centre for Advanced Materials Joining, Canada*
[c] *Fraunhofer Institut für Zuverlässigkeit und Mikrointegration (IZM), Berlin, Germany*

A R T I C L E   I N F O

Article history:
Received 16 February 2009
Received in revised form 27 June 2009
Accepted 3 August 2009
Available online 18 September 2009

Keywords:
Ultrasonic (wedge) bonding
Interface friction
Laser vibration measurement
Tool amplitude
Pad amplitude
Bond process control

A B S T R A C T

The ultrasonic transversal force transmitted to a chip during ultrasonic bonding is derived from measurements of the vibration amplitude at the tool tip and the die edge. To proof the derivation, the transversal force is measured as well by means of a microsensor, which is sensitive to the stress field in the silicon die. The force measured by the microsensor is further referred to as "y-force" To Al-metalized test pads with the integrated microsensors, AlSi1 wire of 25 μm diameter was bonded using a wedge/wedge autobonder. Measurements of the vibration amplitudes and the y-force during bonding were conducted for nine different bonding parameter settings of force and ultrasound (us) amplitude. They confirm a theory for the friction cleaning phase as it was described earlier and will be partially presented here. Compared to earlier measurements of Au-ball-bonds, the results largely show the same behavior and imply that us wedge bonding and thermosonic ball bonding are similar processes. Furthermore, the data approves former interpretations of the bonding process starting with a stiction phase. A clear break off point was found in all pad amplitude measurements, which is followed by a friction plateau that implicates the need of a minimum friction cleaning power.

The discussion made in this paper is interesting for a bond process control system. The transversal force reflects the important stages of the bond process and contains the information to suit as a control signal. But it is impractical to measure the transversal force in situ under the wedge in industrial production, where chip, substrate and bonding table create a complex setup with a high geometric variety. An indirect measurement of the transversal force via the tool tip amplitude opens up new possibilities for gaining an efficient control variable, because the geometry and the properties of the bonding machine are well defined. As a first step it is shown by correlating vibration measurements with microsensor signals, that the tool tip amplitude measured by laser vibrometer contains all of the necessary information needed to control the bond process. From that point, process integrable measurement systems – which are cheaper, more handy and more fail safe than the laser vibrometer – might be developed.

© 2009 Elsevier B.V. All rights reserved.

1. Introduction

With the optimization of wire bonding equipment and test methods, stable wire bonding processes with high throughput and high yields are possible [1]. But the need for smaller systems with higher functionalities can only be satisfied by smaller pitches between two wire connections. Therefore, the process window becomes smaller [2]. To be able to control the process at smaller pitches, variations in bonding tools, wires and surface properties must become smaller as well [3]. Another possibility to compensate for the small process windows would be an in situ bond process control, which is desired by the industry [4–6]. Former models of the ball [7] and wedge [8] bonding process have shown, that the characteristic of the transversal force reveals information about the state of growth of interconnection area $A_{eff}(t)$. Today, the transversal force ($F_T(t)$) measurement with an integrated microsensor [9] is the method which gains information closest at the bonding interface. But in industrial production, it may not be practicable to provide microsensors under the bond pad of a microchip. Hence, indirect measurements of the transversal force using the tool tip and the die edge vibration might be used to get the necessary information about the progression of the process. Measuring the transversal force during bonding by means of a laser vibrometer is the next step towards a bond control that, in the future, can overcome the necessity of parameter optimization and react to strong fluctuations of bond metallization quality by adjusting the us amplitude in situ. Further improvements of such a system can

* Corresponding author.
E-mail address: holger.gaul@tu-berlin.de (H. Gaul).

0167-9317/$ - see front matter © 2009 Elsevier B.V. All rights reserved.
doi:10.1016/j.mee.2009.08.031

replace the laser vibrometer, e.g. by force sensors in the transducer horn.

Since the interfacial welding energy $P_{RR}(t)$ is generated by the friction amplitude $a(t)$ which itself is induced by the tool tip amplitude (a_{tool}), a_{tool} is the closest measure of the energy input to the welding process. It is assumed, that less than 1% of the electrical power is transmitted to the interface for cleaning and activation purposes [10]. The other 99% are lost by the electro-mechanical conversion, the conduction of the us-wave to the interface and vibrations induced into the substrate. It is also known today, that the elastic deformation of the wedge is leading to losses of the friction amplitude $a(t)$ which can change during the bonding process [8]. Changes of the contact geometry might be one reason for the losses, changes of the material properties – e.g. hardness as reported in Refs. [11,12] – might be another explanation. The tool tip vibration amplitude a_{tool} in combination with the transversal force F_T is the welding power input on top of the wedge. This amplitude is thus the best measure of interface friction energy. It provides information about the bond process complementary to the measurement of the transversal force, which is e.g. important for the prediction of the bond growth when comparing experimental results with different bonding parameters [8]. It is necessary to point out here, that up to date the physics of machine characteristic, bond surfaces, and especially of bond parameter influences on a wire bond contact's shearing strength have not been comprehensively described. This paper is an approach to better understand the friction cleaning phase of the bond process. Beyond that stage, the presented theory is not valid. But a better understanding of the creation of the effectively bonded area will provide the basis to a better explanation of the last phase of the bonding process, the diffusion phase.

The main objective of this work is thus, to show that the information of the transversal force, e.g. measured with the microsensor, is contained in the measurements of pad and tool amplitude to apply experiences of the bond process interpretation by theses sizes. In regard of the tool amplitude, it is also an objective to show that a_{tool}, which is on the upward site of the wedge and thus better accessible than the opposite, to the chip allocated site, mirrors the transversal force during the activation stage. If this can be proven, it is clear that a wire bond control can gain every necessary information at the transducer horn, which is very good accessible even in production environments.

2. Theoretical dependencies between vibration amplitudes and transversal forces

Today, the explanation of us-wire bonding by a cleaning procedure due to friction is widely accepted. Fig. 1 shows the details of the bonding process in two characteristics: the us amplitude as the power input (a_0) and the transversal force F_T which shows the characteristic stages of the bonding process. In Point A, the ultrasound begins. It takes some ms for the ultrasound amplitude $a_0(t)$, which is defined as the vibration of the tool for a bonding force $F_{NB} = 0$ cN, to reach the maximum, constant value. During that tuning, the wedge first sticks on the pad (phase a). No friction nor cleaning or bonding can occur in that stage, and the transversal force – defined as the force in direction of ultrasound – increases with the increasing us amplitude. The force is slightly delayed as the mechanical wave needs some time to reach the bonding interface. The friction starts when $F_T(t)$ overcomes the stiction force μ_{Ox} F_{NB} (Point B), where μ_{Ox} is the coefficient of oxide friction (on the uncleaned parts of the interface) and F_{NB} is the bonding force. A clear break-off point – highlighted by an arrow – can be seen in the characteristic of the transversal force $F_T(t)$. The force remains on the level of stiction force for a short time (phase b). The duration

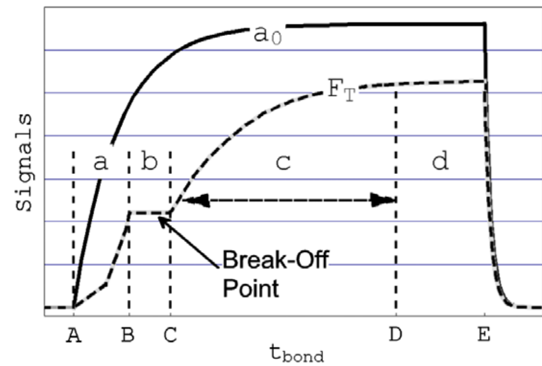

Fig. 1. Detailed explanation of the bonding stages on the basis of $F_T(t)$ using theoretically calculated characteristics of a typical free air vibration. $a_0(t)$ (no bonding) and transversal force (while bonding, bonding force 20 cN). $a_0(t)$: free air vibration (us) amplitude; $F_T(t)$: transversal force. A: start of ultrasound; B: start of friction; C: beginning of friction cleaning; D: end of friction (t_{eof}); E: end of ultrasound. a: stiction phase; b: duration of break-off plateau; c: friction cleaning phase; d: interdiffusion phase.

of that stage is mainly depending on the bond pad surface and the growing us amplitude. It is assumed that wear occurs in this stage. Another explanation might be, that the friction power has to reach a certain level before surface precipitations can be removed from the surface. Cleaning of interfacial surfaces (i.e. growth of the effectively bonded area) starts in Point C, when the transversal force increases strongly for a second time. The increase in the transversal force in the activation phase c is typically lower than in phase a. It is depending on the bond surface and on the bonding parameters ultrasonic power (P_{US}) and bonding force (F_{NB}): The higher the us amplitude and the bonding force are, the faster does the transversal force increase [13]. Cleaning accompanied by bonding lasts until the friction sliding movement of the wedge over the bondpad ends at t_{eof} (end of friction time) and the maximum cleaned area $A_{eff}(t_{eof})$ is reached (D). Afterwards, the transversal force remains constant and the diffusion phase (d) follows, until the ultrasound is switched off (E).

Following the goal of the paper to show the similarity of laser vibration and microsensor signals in the activation stage c, this stage is objective for a detailed analysis now. The upward trend of the transversal force in stage c is explained by the effectively bonded area $A_{eff}(t)$, which is defined as the part of cleaned metals of the interface area $A(t)$ [7]. A_{eff} is growing due to the friction power which is cleaning the interface and caused by the relative movement of the wedge over the bondpad. Where the bonding metals are free from their surface precipitations or oxides and close enough to each other, the coefficient of friction is much higher than at uncleaned areas. In order to calculate the transversal force, a resulting coefficient of friction can be defined, using the coefficient of oxide friction μ_{Ox} and that of metal friction μ_{Met}:

$$\mu_{Res}(t) = (1 - \gamma(t))\mu_{Ox} + \gamma(t)\mu_{Met} \quad (1)$$

$$F_T(t) = \mu_{Res}(t)F_{NB} \quad (2)$$

where $\mu_{Res}(t)$ is the resulting coefficient of friction, $F_T(t)$ is the transversal force, F_{NB} is the bonding force and $\gamma(t)$ is the degree of bonding as defined in Refs. [7,14].

The degree of bonding $\gamma(t)$ as introduced in Ref. [7] represents the fraction of cleaned area $A_{eff}(t)$ in relation to the whole contact area $A(t)$ (see Fig. 2). To calculate the transversal force $F_T(t)$, Amonton's law is used (Eq. (2)). $F_T(t)$ is getting larger with the increasing cleaned area and therefore a measure of the bond growth.

In the following, pad- and tool vibration amplitude according to Fig. 3 are theoretically described. The pad amplitude ($a_{pad}(t)$) is

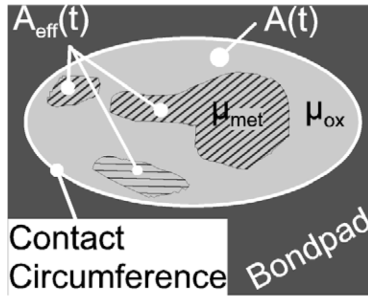

Fig. 2. Schematic of the contact area $A(t)$ and the cleaned area $A_{eff}(t)$ in the bond interface. $A(t)$: time dependent, macroscopic contact area; $A_{eff}(t)$: effectively bonded area; μ_{Ox}/μ_{Met}: friction coefficients of oxide/metal surfaces.

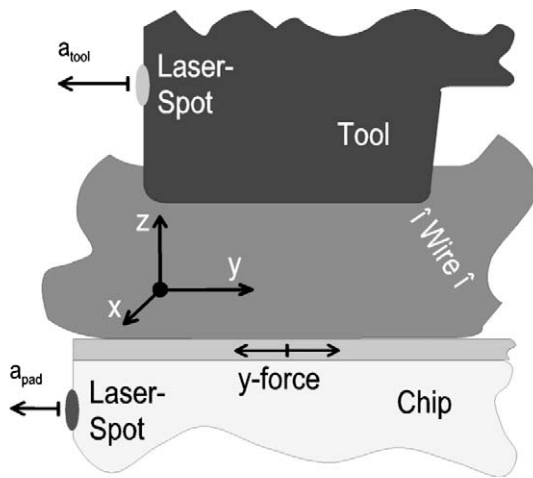

Fig. 3. Schematic explanation of the vibration amplitudes a_n in the setup and the LDV measurement locations (gray spots). a_{tool}: tool vibration amplitude; y-force: microsensor signal; a_{pad}: pad vibration amplitude.

assumed to be proportional to the transversal force $F_T(t)$ and associated to it by the compliance c_{pad}:

$$a_{pad}(t) = c_{pad}F_T(t) \tag{3}$$

The amplitude of the tool tip $a_{tool}(t)$ during bonding can be derived from the free air vibration $a_0(t)$ minus the losses caused by the tool compliance c_{tool}, which represents the attenuation of $a_0(t)$ by $F_T(t)$:

$$a_{tool}(t) = a_0(t) - c_{tool}F_T(t) \tag{4}$$

Based on the friction models for ball bonding [7] and wedge bonding [8], characteristics of $a_{tool}(t)$ and $a_{pad}(t)$ for a typical us-excitation $a_0(t)$ are depicted in Fig. 4. While the pad amplitude is directly proportional to the transversal force, the association of the tool amplitude with the transversal force is emphasized by the gray shaded area, which shows the difference formulated in Eq. (4).

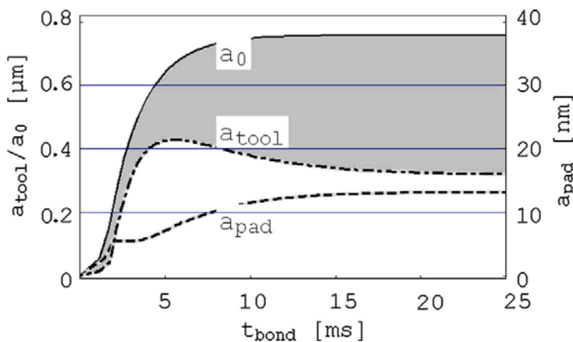

Fig. 4. Theoretically predicted characteristics of a_{tool} and a_{pad}, derived by a_0. a_{tool}: tool vibration amplitude; a_{pad}: pad vibration amplitude; a_0: us amplitude.

3. Experimental setup

To prove Eqs. (3) and (4), bond tests were performed with an F&K Delvotec 6319 w/w bonder. It has an us-generator Uthe 10G with a nominal frequency of 100 kHz and a power output according to Table 1. The substrates were mounted on a vacuum chuck, as shown in Fig. 5. AlSi1 wire with a diameter of 25 μm was bonded. The measurements were made only on the first bond of the loops, and the data was sampled with a rate of 5 MHz while bonding. Afterwards, the signals were filtered to obtain the first harmonic, only the maximum values of the first harmonic of every cycle were stored and are shown here as raw signals in Volt.

In order to be able of measuring the pad amplitude with the Laser Doppler Vibrometer (LDV), the microsensors were mounted in open packages. The die edge and the bondpad were protruding over the package rim, as shown in Fig. 6. There, the AlSi1 loops can also be seen. The asymmetrical loop form guaranteed that only the interesting first bonds are tested in the pull test. Pull and shear tests were made with a Dage4000 tester equipped with either the WP100 or the BS250 measurement cartridge.

The characteristics of tool- and pad amplitude and the y-force were acquired in a random DOE for nine parameter settings. To obtain optimized as well as over- and underbonded samples, the bond parameters were chosen according to Table 2. The samples were bonded at room temperature with a bonding time of 35 ms. To limit the number of measurement with respect to the number of available microsensors, the experiments for the center power (1.b–3.b) and the center bonding force (2.a–2.c) were repeated 10 times. This set of parameter combinations will further be called "cross measurement". The "corner measurement"-parameters were repeated five times each. Thus, 140 bonding experiments

Table 1
US-power output of the generator in arbitrary units (a.u.) and mW. Resulting maximum free air vibration (a_{0max}) of the transducer-tool-system.

US-power [a.u.]	80	100	120
US-power [mW]	330	490	720
a_{0max} [μm]	0.6	0.75	0.9

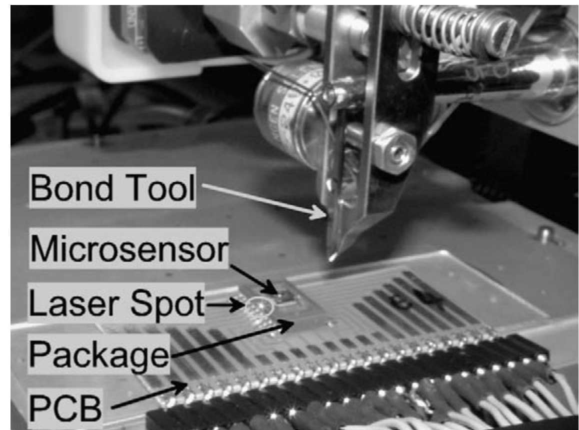

Fig. 5. Mounted sensor in bonding site.

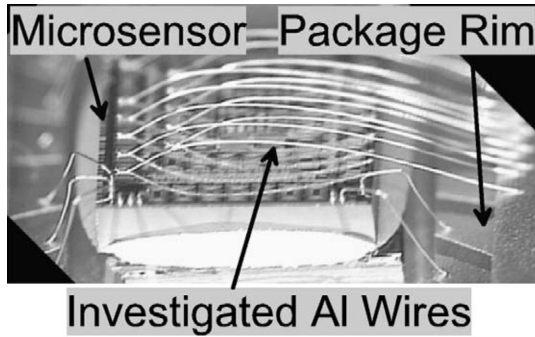

Fig. 6. Microsensor in the package.

Table 2
Bonding parameters for the experiments on Al-microsensors.

/ F_{NB}	P_{US} /	80 [a.u.]	100 [a.u.]	120 [a.u.]
15 [cN]		1.a	1.b	1.c
25 [cN]		2.a	2.b	2.c
40 [cN]		3.a	3.b	3.c

have been made (two times 50 for the cross measurements of tool and pad amplitude, and two times 20 for the corner measurement).

4. Experimental results and discussion

Fig. 7 shows the us-amplitude $a_0(t)$ (measured by the us-voltage), and the three characteristics (a_{tool}, a_{pad}, y-force) over the bonding time in one diagram. Because the microsensor signal is not exactly the transversal force $F_T(t)$, but the stress measured in the silicon die some µm underneath the interface between the wire and the bond pad, the signals measured by the microsensors are further referred to as "y-force". While the us-amplitude tunes in, $a_{pad}(t)$ and the y-force reach the typical break-off plateau as defined in Fig. 1. After approximately 3 ms, the friction starts, clearly distinguishable by the break-off point. From then on, the transversal force remains constant for a few milliseconds, indicating that no cleaned metal surfaces are created by the friction in this stage. There are two explanations for the occurrence of this constant value: wear of interfacial contaminations might be needed to accumulate, before the friction coefficient can grow with the increasing effectively bonded area. A minimum friction amplitude (i.e. minimum friction power in one vibration cycle), which is necessary to remove contaminations, can be another explanation. The minimum size of the particles and the strength of their adhesion determine the amount of needed minimum friction amount of the contaminations. About 2 ms after the break-off point, the resulting friction coefficient (Eq. (1)) is increasing, causing the transversal force to grow, leading to further damping of the tool amplitude, which shows the typical peak value shortly before $a_0(t)$ reaches its maximum magnitude.

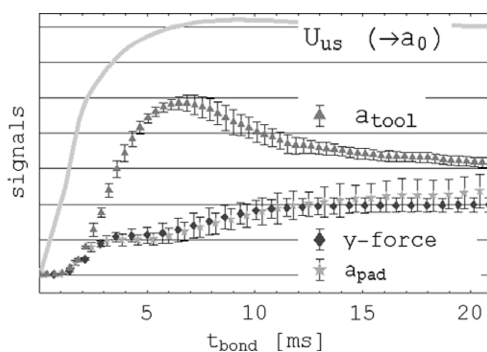

Fig. 7. Example of the measurement of us-voltage, tool and pad amplitude and y-force. Because a_{pad} and the y-force are directly proportional, they appear as one curve. U_{US}: us- (transducer-) voltage (measure for a_0); a_{tool}: tool vibration amplitude; y-force: microsensor signal; a_{pad}: pad vibration amplitude.

The pad amplitude and the y-force, averaged over 10 and five samples for the cross and corner measurements, respectively, are shown in Fig. 8. For each us-power, signals measured with the three bonding forces are shown in one diagram. According to Eq. (2), the transversal force increases with increasing bonding force and with respect to time. The break off point is clearly distinguishable in all pad amplitudes. As expected, the magnitude of the break off point is equal for the three different us-amplitudes at constant bonding force level. The duration of the plateau decreases with increasing us amplitude for all bonding forces.

A possible explanation is that higher us amplitude induces more wear in a shorter time, the surface starts to clean sooner. Another explanation is faster build up of friction with higher US amplitude to overcome minimum friction. During the following stage of bonding, in which the surfaces are cleaned and activated, the pad amplitude and the y-force correlate. It can be seen for all parameter combinations, that the growth rate of transversal force – due to Eqs. (1) and (2) reflecting as well the growth rate of the effectively bonded area – is higher for larger values of the bonding force and us amplitude. When the significant upward trend of the two characteristics ends, the curves show different, non-systematic deviations: The y-force signal reaches constant values for all cross measurements, which might indicate the end of friction cleaning. This observation is in good agreement with measurements of the end of friction cleaning in Refs. [15,16]. Experiments in Ref. [16], where the bond process has been interrupted at different times to check the status of the bond process in correlation to the laser measurements, have shown that the friction cleaning stage ends after the strong rise of the pad amplitude, for all investigated materials and process parameters approximately at 10–15 ms bonding time.

For the corner measurements, sensors with higher sensitivity were used. All corner measurements correlate with an ongoing increase in the pad amplitude. No end of friction is clearly distinguishable there. Possibly, the chip is near one of its resonances in the alignment used for the cross measurements, causing growing pad amplitudes without a further increase in the transversal forces.

The tool tip amplitudes $a_{tool}(t)$ are compared with those derived from the y-force according to Eq. (4) in Fig. 9, named $a_{tool}^{calc}(t)$ (in the same manner as the pad amplitudes). Since $a_{tool}(t)$ is attenuated by the transversal force, it is smaller for higher bonding forces. The peak of $a_{tool}(t)$ becomes narrower for higher bonding forces and us amplitudes, reflecting the increase of bond growth rate as discussed with the pad amplitude/y-force. After the peak, $a_{tool}(t)$ shows a constant drop, which indicates that there is no relative movement between the tool and the wire. This was proven by snapshot images [17], which brought to light tool and wire movement. The images showed that tool and wire are coupled as long as the tool amplitude is decreasing. Only for long bonding times (i.e. overbonded wedges), a relative movement was found which leads to a sudden rise of $a_{tool}(t)$ which afterwards remains constant. For the measurements shown in this paper, it can thus be assumed that there is no relative movement between the tool and the wire.

Here as well, the comparison of $a_{tool}^{calc}(t)$ and $a_{tool}(t)$ shows a good correlation until 10–15 ms bonding time. After that, a_{tool} deviates from $a_{tool}^{calc}(t)$. The difference is largest for high bonding forces (40 cN), where the wedge deformation is high. Fig. 10 shows the wedge widths, measured with a light microscope after the bond process.

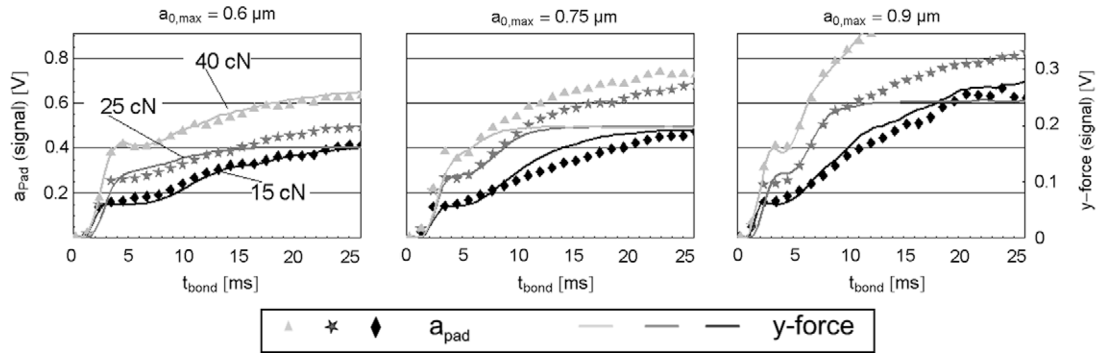

Fig. 8. Correlation of the pad amplitude and the y-force. a_{pad}: pad vibration amplitude; y-force: microsensor signal.

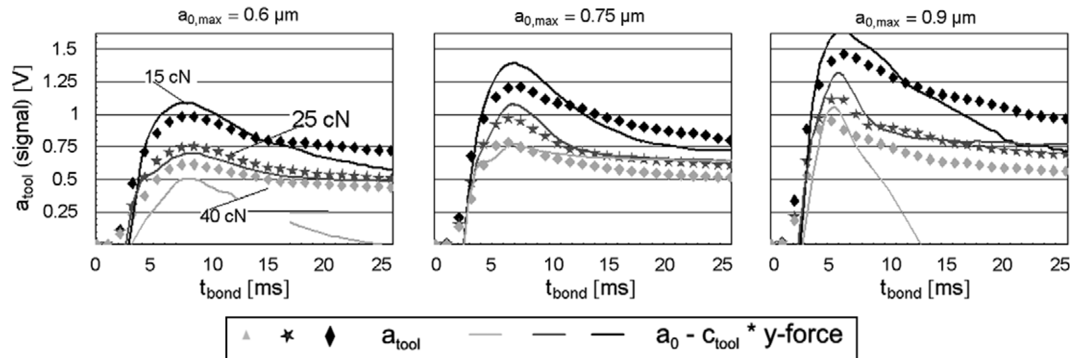

Fig. 9. Correlation of the tool amplitude, as measured and as calculated from the y-force according to Eq. (4). a_{tool}: tool vibration amplitude; y-force: microsensor signal.

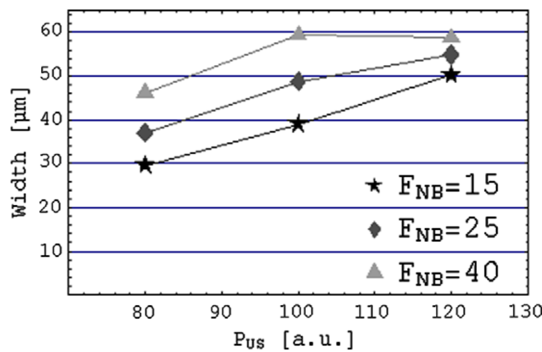

Fig. 10. Wedge widths over us power for the different bonding forces. P_{US}: us power; F_{NB}: bonding force.

The increase of wedge area can result in a tighter coupling of the tool to the wedge and the substrate, so that the tool appears to be stiffer at higher deformation states.

Since the main objective of the work is to show the correlation of the vibration measurements with the microsensor signals, the match of those characteristics shown by Figs. 8 and 9 is proven as well for all 140 measurements by the correlation coefficient r, calculated by:

$$r = \frac{\sum_{k=1}^{N} f_1(t_k) f_2(t_k)}{\sqrt{\sum_{k=1}^{N} f_1(t_k)^2 \sum_{k=1}^{N} f_2(t_k)^2}} 100\%$$

$f_1(t_k)$ and $f_2(t_k)$ are the discrete values of two measurements, in this case $f_1(t_k)$ is the value of the pad amplitude and $f_2(t_k)$ the value of the y-force for $t_{bond} = t_k$ to calculate r_{pad}. For the correlation coefficient r_{tool} a_{tool}, measured by the laser vibrometer, is $f_1(t_k)$ and the tool amplitude derived from the y-force according to Eq. (4) is $f_2(t_k)$. Tables 3 and 4 show the results of this correlation analysis including all measured values up to a bonding time of 15 ms. r_{tool} and r_{pad} have very high values of greater than 97% and thus confirm the analogy of the y-force, the vibration amplitudes and the theory (Eqs. (3) and (4)).

Since it is highly desirable for a bond process control system to measure the transversal force in situ during bonding, the match of the tool tip amplitude a_{tool} and the transversal force F_T opens up new possibilities. According to Eqs. (1) and (2), a control variable proportional to the growth of the bonded interface can be derived from the tool amplitude measured with a laser vibrometer. If the efficiency of such a process monitor can be

Table 3
Correlation of the measured tool amplitudes and the values for the tool amplitude derived from the microsensor measurement up to t_{bond} = 15 ms.

/ F_{NB}	P_{US} /	80 [a.u.]	100 [a.u.]	120 [a.u.]
r_{tool} [%]				
15 [cN]		99.9	99.5	99.9
25 [cN]		97.7	99	98.9
40 [cN]		99.6	97.6	98.9

Table 4
Correlation of the pad amplitude and the y-force up to t_{bond} = 15 ms.

/ F_{NB}	P_{US} /	80 [a.u.]	100 [a.u.]	120 [a.u.]
r_{pad} [%]				
15 [cN]		99.9	98	99.7
25 [cN]		98.1	98.8	99
40 [cN]		98.6	99.97	99.9

shown, further investigations might be spent to replace the expensive and laborious Laser Doppler Vibrometer. To measure the force in the transducer horn by piezo crystals or the tool vibration by acceleration sensors might be possibilities.

5. Conclusions

To prove the assumption of earlier published dependencies between the transversal force and the vibration amplitudes during wire bonding, measurements of the y-force with Al-metalized microsensors, the tool amplitude and the pad amplitude in the same bond process were realized. For the first time, microsensor measurements were performed in Al wedge/wedge bonding. By comparing the time evolution of the measured characteristics, the assumed correlation between the pad amplitude and the y-force as well as the one for the tool amplitude was shown for all parameter settings during the cleaning and bonding phases (i.e. approx. the first 15 ms of the total bonding time). The main objective of the paper was thus approved, and the match of the characteristics was additionally confirmed by calculating the correlation coefficient between pad amplitude and y-force as well as between tool amplitude and the calculated tool amplitude from the y-force for all experiments. As well, this is a further approval of the theoretical description of wire bonding as a friction welding process.

For a bond process control it is desirable to measure the transversal force. It was shown, that the laser measurement of the tool tip amplitude is one possibility which is applicable for all types of chips and substrates. To more precisely derive the transversal force from the tool tip amplitude, further investigations of Eq. (4) are necessary. Deviations in the correlation in Fig. 9 implicate a dependency of the tool compliance from the bonding force and the wedge geometry, respectively.

The data also shows a clear break off point, which is equal for all us-amplitudes (at constant bonding forces), providing that the bond process starts with a stiction phase. Because the us-excitation rises relatively slowly, the transversal force even exhibits a “start of friction”-plateau, as well as a break off point. The plateau can be explained by the need of a minimum friction amplitude (i.e. friction power) in the interface before surface precipitations can be detached.

For the first time, y-force measurements of a w/w bond process and for the material combination Al–Al were made. The acquired curves are similar to those obtained from Au-balls bonded on Al-metallization [7]. The process takes more than two times longer, possibly because of the lower frequency (100 kHz instead of 130 kHz), the slower us tune in and the lower temperatures. It is also possible, that the oxidized AlSi1-wire surface increases the bonding time in comparison to the Au-balls. The experiments have shown in general, that the wedge/wedge bonding process with AlSi1-wire is based on similar physical principles as the ball/wedge bonding process with Au-wire.

The results are showing, how the tool tip amplitude can be used as a command variable which is able to control the us amplitude in order to bond high quality wedges. The interpretation of the bond process by means of the us amplitude $a_0(t)$ and the transversal force $F_T(t)$, necessary for such a control, was given. Further works might show the effectiveness of controlling the bond process by the tool amplitude in order to obtain a desired effectively bonded area of the wedge, and develop a measurement device that will replace the costly laser vibrometer, e.g. force sensors in the transducer horn.

Acknowledgments

The allocation of the microsensors used for the investigations by Oerlikon Esec SA, Cham, Switzerland is greatfully acknowledged by the authors. This research was partly funded by the Natural Sciences and Engineering Research Council (NSERC) of Canada.

References

[1] G.G. Harman, IEEE Transactions on Components, Hybrids and Manufacturing Technology 15 (6) (1992) 1005–1011.
[2] U. Wittenwiler, A. Lateef, J.C. Reiner, Semicon Singapore (2005) 1–9.
[3] G.G. Harman, Wire Bonding in Microelectronics: Materials, Processes, Reliability, and Yield, second ed., Mc Graw-Hill, New York, 1997.
[4] A. Rogado, Wirebond Bond Process Control and Monitoring System, Electronic Materials and Packaging, 2006, EMAP 2006, International Conference on, vol. 8, 2006, pp. 183–222.
[5] W. Scheel, Baugruppen-Technologie der Elektronik: Montage, first ed., Verlag Technik GmbH, Berlin, 1997.
[6] K.P. Galuschki, K.-D. Lang, W. Scheel, VTE – Verbindungstechnik in der Elektronik (1991) 175–180.
[7] M. Mayer, J. Schwizer, Electronics Packaging Technology Conference 5 (2003) 738–743.
[8] H. Gaul, M. Schneider-Ramelow, H. Reichl, Electronics Systemintegration Technology Conference 1 (2) (2006) 719–725.
[9] M. Mayer, Microelectronic Bonding Process Monitoring by Integrated Sensors, Dissertation, Eidgenössisch Technische Hochschule, 2000.
[10] F. Osterwald, Verbindungsbildung beim Ultraschall-Drahtbonden/Einfluß der Schwingungsparameter und Modellvorstellungen, Dissertation, Technische Universität, 1999.
[11] U. Geißler, Verbindungsbildung und Gefügeentwicklung beim Ultraschall-Wedge-Wedge-Bonden von AlSi1 Drähten, Dissertation, Technische Universität, 2008.
[12] U. Geißler, M. Schneider-Ramelow, K. Lang, H. Reichl, Journal of Electronic Materials 35 (1) (2006) 173–179.
[13] H. Reichl, Technologien der Heterosystemintegration: Skript zur Vorlesung, TU-Berlin, Technische Universität Berlin, SS2008.
[14] M. Mayer, J. Schwizer, Proceedings of the Semicon Singapore (2002) 169–175.
[15] H. Gaul, M. Schneider-Ramelow, H. Reichl, Microsystem Technologies 15 (5) (2009) 771–775.
[16] H. Gaul, Berechnung der Verbindungsqualität beim Ultraschall-Wedge/Wedge-Bonden, Dissertation, Technische Universität, 2009.
[17] H. Gaul, M. Schneider-Ramelow, H. Reichl, Hochgeschwindigkeitsaufnahmen der Werkzeug- und Drahtschwingung beim US-Wedge/Wedge-Bonden, Produktion von Leiterplatten und Systemen 8, 2007, pp. 1529–1534.